

Heterogeneous catalytic solvent-free synthesis of 3,3,5-trimethyl cyclohexyl anthranilic acid esters via transesterification

Chittaranjan S. Thatte¹ · Manapragada V. Rathnam¹ · Ashutosh Namdeo² · Kiran Rane¹

Received: 12 June 2016 / Accepted: 5 October 2016
© Institute of Chemistry, Slovak Academy of Sciences 2016

Abstract The transesterification of anthranilates with both mixtures of cis and trans and pure trans 3,3,5-trimethyl cyclohexanol was studied using ‘calcium-oxide- and magnesium-oxide’-based catalysts under ‘solvent-free’ conditions. The catalysts were characterized by XRD, CO₂-TPD, BET-surface area, and FEG-SEM analysis. Pure calcium oxide was found to be the most effective heterogeneous catalyst. Pure ‘calcium-oxide’-based catalyst was recycled five times without appreciable loss in the catalytic activity. The TOF after five recycles was 10.7 mol/mol of catalyst/h. The study was further extended for the synthesis of new anthranilates. The synthesized pure esters have been characterized by UV-Vis, IR-, ¹H NMR-, and ¹³C NMR spectroscopies and mass spectrometry.

Keywords Transesterification · Methyl anthranilate · Trimethyl cyclohexanol · Calcium oxide · Mixed magnesium-calcium oxide

Electronic supplementary material The online version of this article (doi:10.1007/s11696-016-0061-z) contains supplementary material, which is available to authorized users.

✉ Manapragada V. Rathnam
mvrathnam58@rediffmail.com

Chittaranjan S. Thatte
chittthatte@gmail.com

Ashutosh Namdeo
ashutoshtnamdeo83@gmail.com

Kiran Rane
kiranrane8@gmail.com

¹ Chemistry Research Laboratory, B. N. Bandodkar College of Science, Chendani Bunder Road, Thane 400601, India

² Chemical Engineering Division, CSIR-North East Institute of Science and Technology, Jorhat, Assam 785006, India

Introduction

Transesterification is one of the classic organic reactions that have enjoyed numerous laboratory uses and industrial applications. The ester-to-ester transformation is particularly useful when the parent carboxylic acids are labile and difficult to isolate. Transesterification with heterogeneous catalyst serves as green and useful means to synthesize higher homologues of esters. Metal alkoxides (Taft et al. 1950; Billman et al. 1947; Haken 1966; Frank et al. 1944; Wulfman et al. 1972; Rossi and de Rossi 1974), aluminum isopropoxide (Rehberg and Fisher 1947; Brenner and Huber 1953), tetraalkoxytitanium compounds (Seebach et al. 1982; Imwinkelried et al. 1987; Blandy et al. 1991), and organotin alkoxides (Otera et al. 1986) are applied as catalysts for transesterification reactions. Heterogeneous catalysts, such as alkylguanidines (Sercheli et al. 1999), attached to modified polystyrene or siliceous MCM-41, Na/NaOH/-Al₂O₃ (Kim et al. 2004), tin complex [Sn(3-hydroxy-2-methyl-4-pyrone)2(H₂O₂)] (Abreu et al. 2005) ZrO₂, ZnO, SO₄²⁻/SnO₂, SO₄²⁻/ZrO₂, KNO₃/KL zeolite and KNO₃/ZrO₂ (Jitputti et al. 2006), potassium loaded on alumina (Xie et al. 2006), potassium loaded on a mesoporous MSU-type alumina, KF, LiF and CsF (Verziu et al. 2009), and KF/ZnO (Hameed et al. 2009). Heteropolyacid (Cs_{2.5}H_{0.5}PW₁₂O₄₀) (Zhang et al. 2010), Cs-exchanged NaX faujasites, a commercial hydrotalcite, magnesium oxide, and barium hydroxide (Leclercq et al. 2001) have been used.

Among the heterogeneous catalysts used, generally, calcium oxide (CaO) is a candidate for the solid base catalyst from an economical point of view and it has been used as a catalyst on several occasions (Kouzu and Hidaka 2012; Boeya et al. 2011). In this work, we have used co-

precipitated calcium oxide and calcium oxide–magnesium-oxide-type mixed catalyst.

3,3,5-Trimethyl cyclohexanol (3,3,5-TMCH) finds application in the preparation of perfumes. However, its major application is in preparation of various derivatives, such as acetates and salicylate for cosmetic applications (Gambaro et al. 2006). The salicylic acid ester of 3,3,5-TMCH has been reported for sunscreen properties. The esterification of salicylic or anthranilic acid ester has been attempted. However, there are no reports of the transesterification methodology involving the use of 3,3,5-TMCH and anthranilic acid ester. It was, therefore, of interest to study the transesterification reaction of 3,3,5-TMCH and anthranilic acid esters using various acidic and basic catalysts. The transesterification was eventually extended for the synthesis of novel potential sunscreens using calcium oxide as a solid base heterogeneous catalyst, which has not been reported in the literature.

Experiment

Materials

All the reagents used for the preparation of catalysts and for the synthesis and analysis of catalytic activity were pure and procured from E Merck., Aldrich, and SD fine chemicals. Commercially available grades of mix (cis + trans ratio 85:15) 3,3,5-trimethylcyclohexanol and pure trans-3,3,5-trimethylcyclohexanol (99% pure) were procured from SI-Group (I) Ltd (will be termed in this paper henceforth as mix TMCH and pure trans TMCH, respectively).

Techniques

Gas chromatograph (Agilent 6890) with FID and Varian CP 8934 capillary column (10 m length, 100 μm diameter, and 0.40 μm film thickness) was used to establish the separation of geometrical isomers with GC parameters, such as oven, 100–45 $^{\circ}\text{C}/\text{min}$ –280 $^{\circ}\text{C}$ —2 min hold, inlet, 250 $^{\circ}\text{C}$, detector 300 $^{\circ}$, split ratio 1:500, and sample injection 0.2 μl .

The XRD analysis of the catalysts was performed using X'pert Pro (from P analytical) at a wavelength of 260–850 nm. The FT-IR characterization was performed using Vertex 80 FT-IR System. Temperature-programmed desorption (TPDRO 1100, Thermo Scientific) of carbon dioxide (CO_2 -TPD) was used to determine the base properties of catalysts. Before the analysis, samples were pretreated. In a typical pretreatment procedure, the gas line was first cleaned by inert gas (Argon), and then, the sample was exposed to Argon at higher temperature (800 $^{\circ}\text{C}$) with

higher flow rate 50 ml/min to ensure that the exposed catalyst surface is free from the moisture if any.

After the pretreatment sample was saturated with the CO_2 pulses followed by the TPD performed up to 800 $^{\circ}\text{C}$ under helium flow (20 ml min^{-1}). All areas of sub-peaks were summed to calculate the total amount of base sites. ^1H NMR and ^{13}C NMR of the pure compounds were determined using VARIAN 300 MHz USA. Elemental analysis was performed using Flash EA-1112 Series instrument. BET-surface area was determined using Tristar 3000 V 6.05 A using nitrogen adsorption.

Catalyst preparation

In the present work, three types of catalysts were prepared. Catalyst-a is the calcium-oxide-based catalysts prepared using literature methods (Kontoyannis and Vagenas 2000; Galmarini et al. 2011) by co-precipitation of calcium nitrate with sodium carbonate, whereas catalyst-b and catalyst-c are mixed calcium-oxide–magnesium-oxide-based catalysts.

Method for the preparation of catalyst-a

In a typical procedure for the preparation of catalyst-a, 34.74 g (0.21 mol) of calcium nitrate was dissolved in 50 ml of distilled water, and the solution was heated to 100 $^{\circ}\text{C}$ under efficient stirring. A solution of sodium carbonate 23 g (0.21 mol) in 50 ml of distilled water was added to this solution within 20 min. The mixture was cooled after complete precipitation of calcium carbonate. It was filtered, dried for 3 h at 120 $^{\circ}\text{C}$, and calcined at 950 $^{\circ}\text{C}$ for 5 h. Theoretical wt% (CaO 100%).

Method for the preparation of catalyst-b

For the preparation of catalyst-b, solution containing 23.43 g (0.14 mol) of calcium nitrate in 25 ml of distilled water and magnesium nitrate 21.07 g (0.14 mol) dissolved in 25 ml of distilled water was heated to 100 $^{\circ}\text{C}$ under efficient stirring. A solution of sodium carbonate 30.19 g (0.28 mol) dissolved in 100 ml of distilled water was added to this solution within 20 min. The mixture was cooled after complete precipitation of mixed calcium carbonate–magnesium carbonate. The precipitate was filtered, dried for 3 h at 120 $^{\circ}\text{C}$, and calcined at 950 $^{\circ}\text{C}$ for 5 h. Theoretical wt% of mixed CaO (58.2):MgO (41.8).

Method for the preparation of catalyst-c

For the preparation of catalysts-c, solution containing 32.82 g (0.20 mol) of calcium nitrate dissolved in 35 ml

of distilled water and magnesium nitrate 11.69 g (0.079 mol) dissolved in 15 ml of distilled water was heated to 100 °C under efficient stirring. A solution of sodium carbonate 30.19 g (0.28 mol) dissolved in 100 ml of distilled water was added to this solution within 20 min. The mixture was cooled after complete precipitation of mixed calcium carbonate–magnesium carbonate. The precipitate was filtered, dried for 3 h at 120 °C, and calcined at 950 °C for 5 h. Theoretical wt. % of mixed CaO (77.85): MgO (22.15).

Catalytic tests

Reaction procedure

The transesterification reaction, as shown in Fig. 1, was carried out in a 100 ml R.B. flask with a stirrer, condenser, thermometer pocket, and dean and stark separator. Initially, mix TMCH was mixed with catalyst under stirring with a rate of 600 rpm. The mixture was heated to 190 °C when methyl anthranilate was added for the period of 20 min. After complete methanol liberation (typically 1 h), the contents were cooled and the reaction sample was analyzed by gas chromatography. The conversion and selectivity for each prepared catalyst were studied. The catalyst was recycled five times after washing with acetone, drying at 100 °C, and calcinations at 750 °C.

Results and discussion

Characterization of catalysts

The prepared catalysts were characterized by powder XRD, elemental analysis, FEG-SEM analysis, and CO₂-TPD.

XRD Analysis: From the XRD patterns shown in Fig. 2, it can be observed that the catalyst-a showed typical diffraction peaks due to 100% CaO at $2\theta = 32.40^\circ$, $2\theta = 37.66^\circ$, $2\theta = 54.15^\circ$, $2\theta = 64.41^\circ$, and $2\theta = 67.66^\circ$. These diffraction peaks of CaO are similar to previously published results (Watcharathamrongkul et al. 2010). The catalyst-b showed extra peak due to MgO (He et al. 2010) at $2\theta = 43.23^\circ$ and $2\theta = 62.49^\circ$ in addition to the peaks due to CaO. The catalyst-c also showed the extra peak due to MgO at $2\theta = 43.04^\circ$ and $2\theta = 62.43^\circ$, but in the case of catalyst-c, the peak was less intense, indicating a subsequent reduction in the composition of MgO (22.15 wt%) compared with the catalyst-b (41.8 wt%). Diffraction peak at $2\theta = 35^\circ$ was due to the formation of calcium hydroxide after moisture absorption, which followed the order of intensity $b > a$.

FT-IR spectra of the catalysts

FT-IR spectra of catalysts were recorded to examine the influence of change in calcium oxide composition, as shown in Fig. 3. The background spectrum was recorded at ambient temperature and was compensated during the

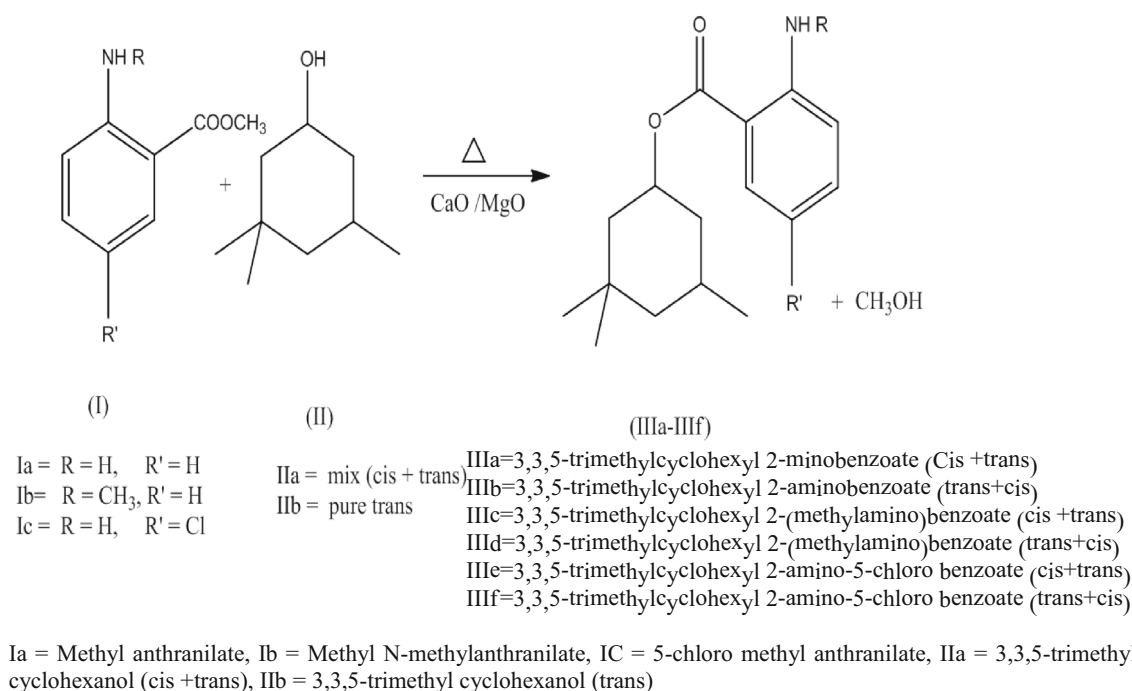


Fig. 1 Synthesis of 3,3,5-trimethyl cyclohexyl anthranilic acid esters by transesterification

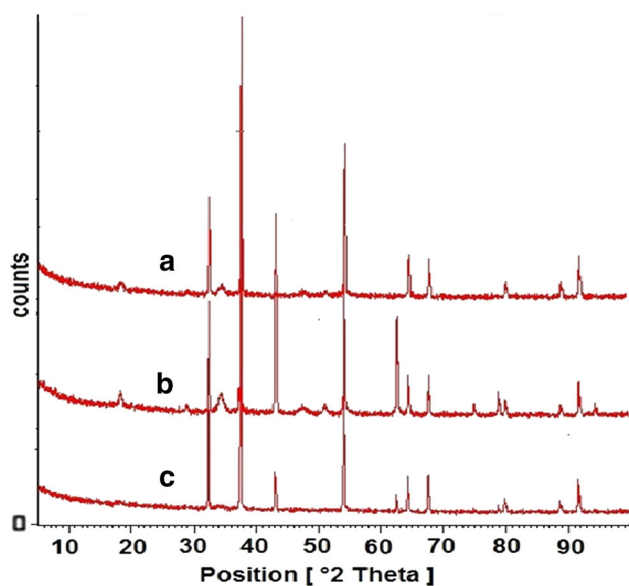


Fig. 2 XRD analysis of catalysts: *a–c*

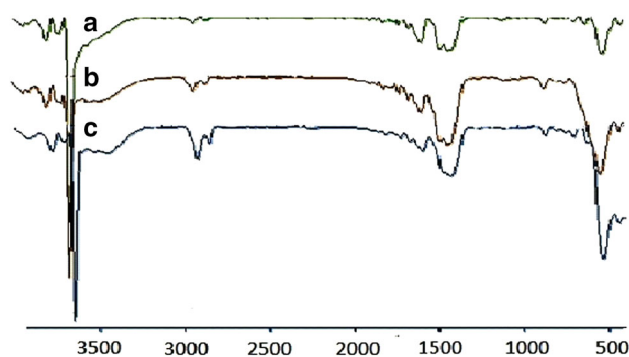


Fig. 3 FT-IR spectra of catalysts *a, b, and c*

sample run under atmospheric condition. The spectra were recorded without any pretreatment of the prepared catalyst.

Catalysts *a, b, and c* showed bands at 1413, 1437, 1429, 870.75, 876.27, and 870.84 cm^{-1} which can be attributed to absorb CO_2 and bands at 3639, 3642, and 3642 cm^{-1} are due to absorbed water in the calcium oxide and calcium oxide–magnesium oxide samples (Dan et al. 2001). The difference in the intensity of absorption bands due to absorption of carbon dioxide (see Fig. 3); in case of catalysts *a, b, and c* at 1480, 1474, and 1472 cm^{-1} . The intensity of absorbance follows the order catalyst-*b* > catalyst-*a* > catalyst-*c*. The catalyst with high concentration of magnesium oxide, i.e., catalyst-*b*, is quite sensitive towards the atmospheric absorption of carbon dioxide than catalysts *a* and *c*. We also found a difference in the intensity of absorbed moisture in the catalysts. Catalyst-*b* has more intensity of the band at 3642 cm^{-1} compared to that of catalysts *a* and *c*. Therefore, it can be inferred that catalyst with higher concentration of MgO (catalyst-*b*) will show more tendency towards the

absorption of water compared to the catalyst with less concentration of MgO (catalysts *a* and *c*). The intensity of absorption bands due to water was in the order *b* > *a* > *c*.

CO_2 -TPD of catalysts

The alkalinity (basic nature) of the catalysts was measured using CO_2 -TPD technique. The CO_2 -TPD profiles of catalysts are shown in Fig. 4. The catalysts were subjected to the test under the conditions mentioned in the experimental section. The amounts of base sites in the catalysts, as summarized in Table 1, are calculated from the area below the curve of TPD profiles. The characteristic peaks of these TPD profiles are assigned to their desorption temperatures indicating the strength of base sites. From CO_2 -TPD profiles (Fig. 4), the CO_2 desorption peaks appear in all profiles at high temperature (≥ 650 °C) suggesting that the catalysts have strong base sites (see Fig. 4).

In all cases except catalyst-*b*, single desorption peak was observed. In case of the catalyst-*b*, two desorption peaks were observed (643 and 800 °C). However, for catalyst-*b*, 643 °C is the major and contributing peak as it represents 73.6% of the peak area (Fig. 4). The order of base sites of the catalysts after calculations is *a* > *c* > *b*. The basicity increased with the increase in the amount of calcium oxide; hence, the order of basicity was found to be 100% CaO > CaO:MgO,(77.85:22.15) > CaO:MgO,(58.2:41.8).

FEG-SEM analysis of catalysts

FEG-SEM were carried out to see the morphology of the catalysts. Catalysts *b* (Fig. 6) and *c* (Fig. 7) are mixed MgO/CaO catalysts, which showed finer particle size compared to catalyst-*a* (Fig. 5), which is a pure calcium oxide catalyst.

A number of heterogeneous and homogeneous catalysts, such as potassium carbonate, sodium carbonate, barium hydroxide, hydrotalcite, calcium oxide, magnesium oxide, zinc oxide, aluminum oxide, sodium methoxide, potassium tertiary butoxide, and sodium hydroxide, were initially screened for the transesterification. Sodium methoxide, potassium carbonate, and calcium oxide were found to be active. Owing to the reusability limitation of first two catalysts, calcium oxide was found to be the most effective and advantageous heterogeneous catalyst for the transesterification. Hence, the reaction was only studied using calcium-oxide-based catalyst. Table 2 shows the conversion and selectivity data. The selectivity values for the product have been expressed independently as values of *cis* and *trans* isomers. It was observed that the reaction is much faster when homogeneous alcoholic sodium hydroxide was used (Entry 7); however, the product selectivity remained the same as compared with the reaction with heterogeneous

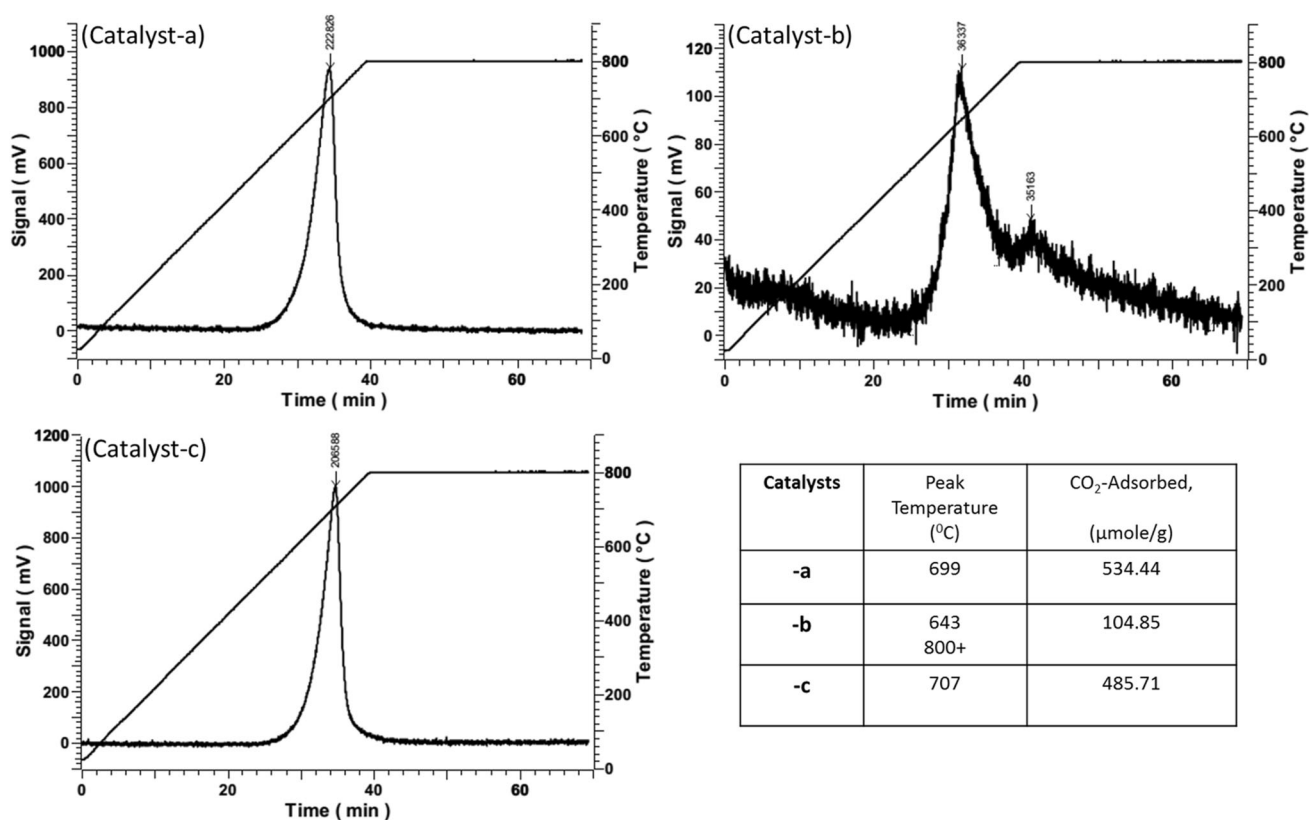


Fig. 4 CO₂-TPD of catalysts *a*, *b*, and *c* (+ represent that a peak observed at the very beginning of the holding temperature 800 °C during the TPD analysis)

Table 1 BET-surface area and base sites of catalysts

Catalysts	BET-surface area (m ² /g)	Base sites (μmole/g)
a	2.619	534.44
b	12.91	104.85
c	5.742	485.71

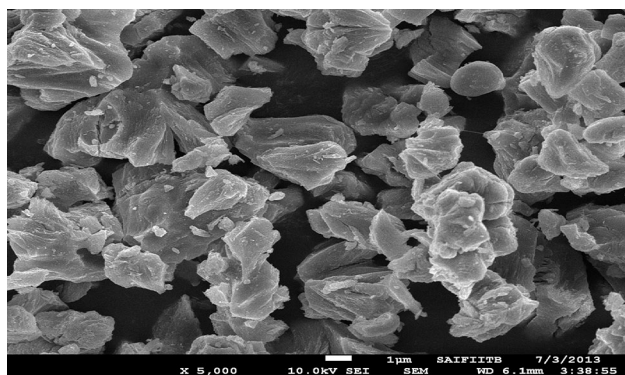


Fig. 5 FEG-SEM image of catalyst-a

calcium oxide (Entry 9). It is observed from the reaction data that pure *trans* 3,3,5-TMCH (Fig. 1, IIb) has less reactivity compared with the mixed 3,3,5-TMCH (Fig. 1,

IIa) under otherwise the same reaction conditions (Entry 12, 14, 16). When mix alcohol (IIa) is used in combination with the electron donating substituent on the ester tend to decrease the conversion (Entry 13), whereas electron withdrawing group on the ester has a positive effect on the conversion (Entry 15). In all the cases, some (*cis*) product formations were also observed when the reaction was conducted with pure *trans* 3,3,5-TMCH (IIb). Catalyst-a was recycled five times without a significant loss in catalytic activity. Each time the catalyst was washed with acetone, oven dried at 100 °C, and calcined at 750 °C and then reused. This has been represented graphically in terms of TOF in Fig. 8.

Effect of molar ratio of alcohol to ester on conversion and selectivity

The effect of molar ratio of alcohol to ester on transesterification using catalyst-a has been presented graphically in Fig. 9. The molar ratio was studied at four points 2,3,4,5 using Ia and IIa. During this study, the temperature, catalyst loading, and other parameters, such as stirring rate, were kept constant. At a higher mole ratio 5, the conversion was the highest (99.2) and the selectivity was the lowest (97.6). In lower mole ratio 2, the conversion was (95.7) and

Table 2 Conversion and selectivity of different 3,3,5-trimethyl cyclohexyl anthranilates

Entry	Ester used	Alcohol used	Catalyst used	Time (min)	% Conversion	% Product selectivity		% Yield (i)
						cis	trans	
1	Ia	IIa	No catalyst	60	No reaction	–	–	
2	Ia	IIa	Na ₂ CO ₃ [§]	600	30.7	82.6	5.5	–
3	Ia	IIa	K ₂ CO ₃ [§]	120	98.6	88.0	10.0	–
4	Ia	IIa	NaOMe [§]	600	94.5	90.3	7.0	–
5	Ia	IIa	MgO [§]	600	94.2	91.0	8.0	–
6	Ia	IIa	KOBu-t [§]	180	46.0	90.6	9.3	–
7	Ia	IIa	NaOH ^{*, †}	20	98	92.0	6.2	74.2
8	Ia	IIa	KOH ^{*, †}	60	72.1	88.9	8.9	–
9	Ia	IIa	a [†]	60	95.8	91.8	6.3	72.0
10	Ia	IIa	b [†]	60	79.6	91.9	5.7	–
11	Ia	IIa	c [†]	60	91.6	91.4	6.7	–
12	Ia	IIb	a [†]	120	73.1	12.1	84.9	63.5
13	Ib	IIa	a [†]	120	86.6	91.4	5.3	80.2
14	Ib	IIb	a [†]	540	82.5	15.9	80.0	74.5
15	Ic	IIa	a [†]	120	89.2	92.9	6.4	79.2
16	Ic	IIb	a [†]	240	55.1	8.97	86.83	42.3

Reaction conditions: mole ratio of alcohol/ester = 2

% Conversion = [(% of ester consumed)/(% of ester taken)] × 100

% Selectivity = [(% of product)/(100 – sum of % of reactants)] × 100

(i) = isolated yield

[†] Catalyst concentration g/total mole of reactants = 2.9, temperature = 190 °C

* Alcoholic solution

[§] Catalyst concentration used, g/total mole of reactants = 5.8

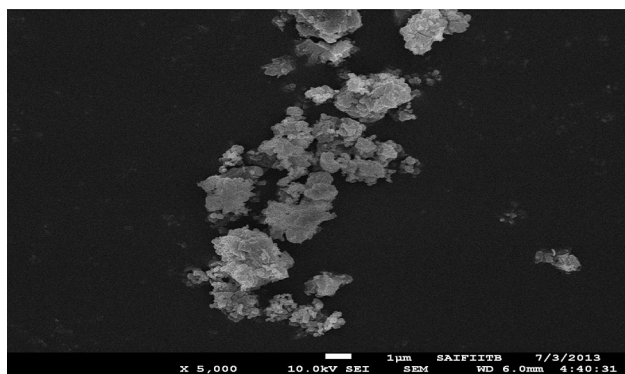


Fig. 6 FEG-SEM image of catalyst-b

selectivity was (98.1). It can be concluded from the study that the higher molar ratio improves the conversion but marginally reduces the selectivity.

Effect of catalyst loading on conversion and selectivity

Effect of catalyst loading was studied at four different loadings, such as 1.7, 2.2, 2.6, and 2.9 g/total moles of

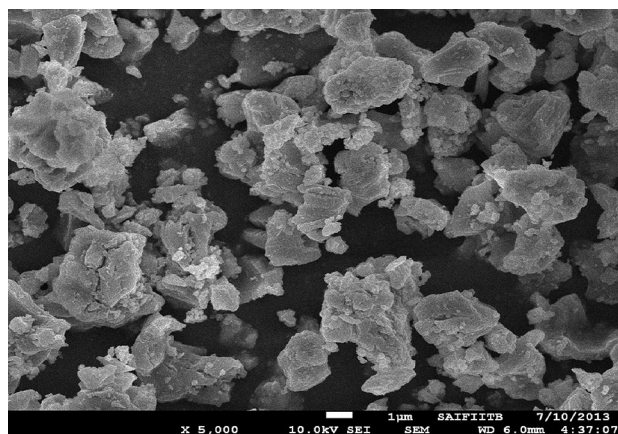


Fig. 7 FEG-SEM image of catalyst-c

reactants (Fig. 10), maintaining the rest of the reaction conditions, such as temperature, mole ratio, and rate of stirring constant. We observed that the conversion increased when the catalyst amount was increased from 1.7, 2.2, 2.6, and 2.9 g/total mole of reactants (Fig. 10). At 2.9 g/total moles, reactants loading the conversion are the highest (98.4); however, the selectivity values observed to

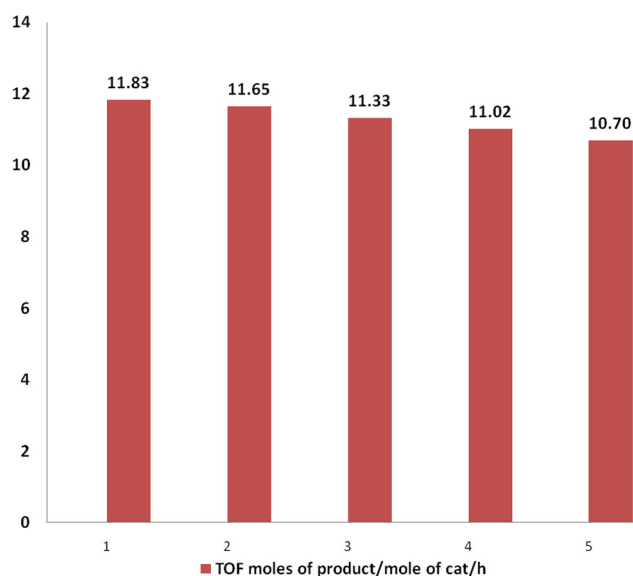


Fig. 8 TOF of during five recycles, TOF after five recycles = 10.7

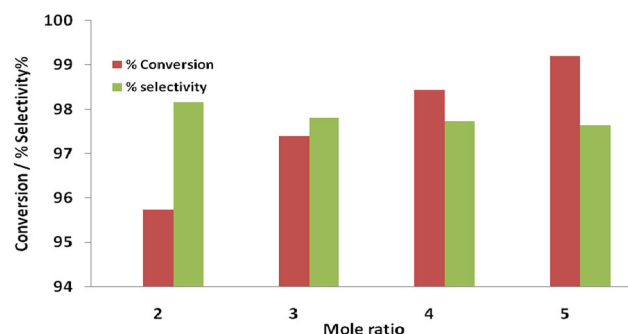


Fig. 9 Effect of mole ratio on % conversion and % selectivity of product. Reaction conditions: catalyst concentration g/total moles of reactants = 2.9, temperature 190 °C, time = 1 h

be marginally high (97.7). At lower catalyst loading (1.7 g/total moles of reactants), the conversion was found to be (96.51) and the selectivity was found to be (97.6). It can be inferred that, as the catalyst loading is increased, there is rise in conversion but marginal increase in selectivity. From Fig. 10, it seems that there is a liner increase in the conversion up to catalysts loading 2.6 g/total moles of reactants, and furthermore, it is deviated from the linearity. Therefore, from this experiment, we found 2.6 g/total moles of reactants as an optimum catalyst loading for the reaction.

Effect of temperature on conversion and selectivity

Effect of temperature was studied at five different temperatures. Table 3 shows the conversion obtained at the corresponding temperatures. As a result, 190 °C was chosen as a final reaction temperature.

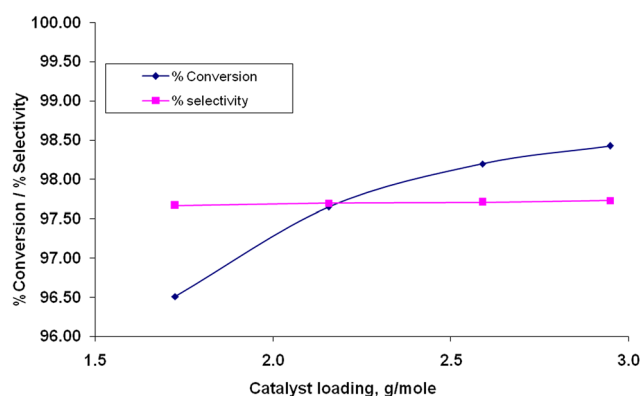


Fig. 10 Effect of catalyst loading on % conversion and % selectivity of product. Reaction conditions: mole ratio = 2, temperature 190 °C, time = 1 h

Table 3 Effect of temperature on % conversion

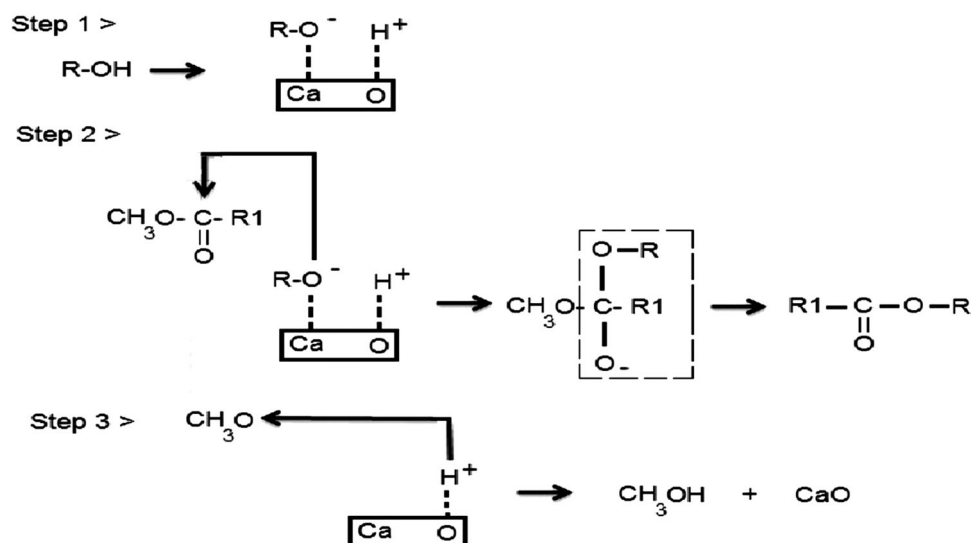
Temperature	% Conversion
150	4
160	6
170	9
180	30
190	95.7

Reaction conditions: mole ratio = 2, catalyst load = 2.9 g/total, moles of reactants, time = 1 h

Following Tables 4 and 5 show characterization data of compounds IIIa and IIIb

Mechanism of transesterification

The mechanism of transesterification with 3,3,5-TMCH and methyl anthranilate using solid basic calcium oxide catalyst at higher temperature is quite comparable to the mechanism of transesterification of oil using calcium oxide as a catalyst (Kouzu and Hidaka 2012). It involves abstraction of proton from alcohol by the basic sites to form cyclohexoxy anion, which is the first step of the reaction. The cyclohexoxy anion attacks carbonyl carbon in a molecule of the methyl anthranilate, leading to the formation of the cyclohexoxy carbonyl intermediate. Then, the cyclohexoxy carbonyl intermediate divides into two molecules, the product and the methoxy anion. Figure 11 illustrates a mechanism on the catalyzed transesterification using calcium oxide as a solid base. Although the BET-surface area of the magnesium-oxide-based prepared catalysts b and c is high compared with the pure calcium-oxide-based catalyst, it can be emphasized on the basis of the conversion data using all three catalysts that the nucleophilic reaction was accelerated by an enhancement of the basic properties.

Fig. 11 Mechanism of transesterification**Table 4** Characterization of compounds

Compound	Formula	M_r	w_i (calc.)/%			Yield (%)	M.p/B.p. (°C)
			w_i (found)/%				
			C	H	N		
<i>IIIa</i>	$\text{C}_{16}\text{H}_{23}\text{NO}_2$	261.36	73.63	8.87	5.36	72.03	60.1/189
			73.60	8.85	5.35		10 mb Hg
<i>IIIb</i>	$\text{C}_{16}\text{H}_{23}\text{NO}_2$	261.36	73.63	8.87	5.36	63.53	196
			73.61	8.84	5.33		18 mb Hg

Table 5 Spectral data of compounds

Compound	Spectral data
<i>IIIa</i>	<p>U.V, λ/nm: 253 (benzenoid form), 322, 356 (fine structure band)</p> <p>IR, $\tilde{\nu}/\text{cm}^{-1}$: 1247 (CN), 1469 (aromatic), 1596 (NH bend primary amine), 1668(C=O), 2943 (CH stretch alkyl), 3370 (NH stretch), 3483(aromatic primary amine)</p> <p>^1H NMR (CDCl_3), δ: 0.781–0.893(m, 1H, a), 0.913–0.935(m, 3H, b), 0.967–0.985 (m, 6H, c, d), 0.999–1.2 (m, 1H, e), 1.18–1.3(m, 1H, f), 1.34–1.39(m, J 3.29, 1H, g) 1.7–1.82(m, 2H, h, i), 2.09(m, 1H, j), 5.1(dddd, J_1 4.44, J_2 9.0, J_3 11.70, J_4 16.2, 1H, k), 5.6 (s, 2H, l) D_2O exchangeable, 6.582–6.605 (dd, J_1 1.50, J_2 5.55 1H, m), 6.61–6.65 (m, 1H, n), 7.18–7.254(m, 1H, o), 7.823–7.870(dd, J_1 1.65, J_2 8.54 1H, p)</p> <p>^{13}C NMR ($\text{DMSO}-d_6$), δ: 28.3 (CH_2), 129.4 (C), 131.1 (C), 164.2 (CO)</p> <p>ESI positive mode 262.17 (M+H), $\text{C}_{16}\text{H}_{23}\text{NO}_2$</p>
<i>IIIb</i>	<p>U.V, λ/nm: 255 (benzenoid form), 322, 360 (fine structure band)</p> <p>IR, $\tilde{\nu}/\text{cm}^{-1}$: 3482(aromatic primary amine), 3369 (NH stretch), 2937 (CH stretch alkyl), 1682(carbonyl), 1597 (NH bend primary amine), 1467, (aromatic ring), 1248 (CN stretch)</p> <p>^1H NMR spectrum of IIIb in (CDCl_3, 300 MHz) showed signals at 0.79–0.99(m, 7H, a, b, c), 1.01–1.2(m, 4H, d, e) 1.33–1.40(dd, J_1 3.6, J_2 15.0 1H, f) 1.45–1.522(m, 1H, g), 1.76–1.97(m, 3H, h, i, j), 5.3(dd, J_1 2.99, J_2 6.0, J_3 9.3 1H, k), 5.4(bs, 2H, l) D_2O exchangeable, 6.59–6.66(m, 2H, m, n), 7.206–7.271(m, 1H, o), 7.850 (dd, J_1 1.50, J_2 8.40, 1H, p)</p> <p>^{13}C NMR (CDCl_3, 75.5 MHz) 22.58 (a), 23.62 (b), 27.63 (c), 30.60 (d), 34.02 (e), 38.61 (f), 41.62 (g), 48.20 (h), 71.06 (i), 111.56 (j), 116.29 (k), 116.76 (l), 131.14 (m), 133.85 (n), 150.63 (o), 167.75</p> <p>ESI positive mode 262.20 (M+H), $\text{C}_{16}\text{H}_{23}\text{NO}_2$</p>

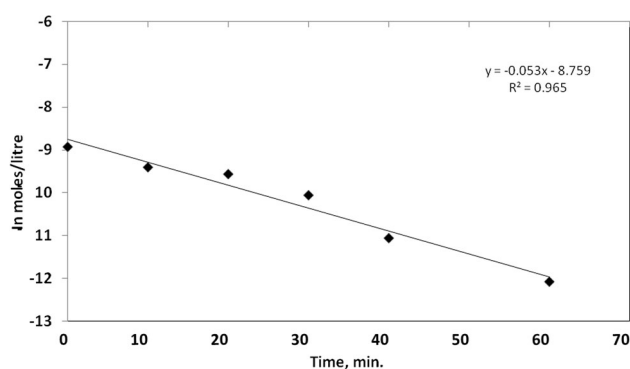


Fig. 12 Kinetics of transesterification of 3,3,5-trimethyl cyclohexanol and methyl anthranilate. Reaction conditions: mole ratio of alcohol/ester = 2, catalyst concentration g/total moles of reactants = 2.9, temperature 190 °C

Kinetics of transesterification of methyl anthranilate with 3,3,5-trimethyl cyclohexanol

The reaction follows the first-order kinetics with methyl anthranilate under the optimized reaction conditions (Fig. 12). From the kinetic plot of experimental data, the first-order rate constant— k —was calculated as shown in Fig. 12. The first-order rate constant for the transesterification with catalyst-a was measured as $0.053 \text{ mol l}^{-1} \text{ h}^{-1}$.

Conclusions

All the mentioned catalysts were prepared by co-precipitation method and characterized by various techniques, such as XRD, CO_2 -TPD, FEG-SEM image analysis, and BET. XRD analysis reveals the crystalline phase of the catalysts. Based on the intensity of calcium hydroxide peak, it can be inferred that catalyst with higher concentration of MgO (catalyst-b) showed more tendency towards the absorption of water compared with the catalyst with less concentration of MgO (catalyst-c). The catalytic activity was in the order of $a > c > b$, which was also in agreement with the basicity of the catalysts. The catalyst 'a' was recycled five times without appreciable loss in the catalytic activity. The highest conversion (95.8%) and selectivity (98%) of the ester were obtained when catalyst-a was used to catalyze the reaction of Ia and IIa. The TOF after five recycles was 10.7 mol/mol of catalyst/h. The higher molar ratio was effective in improving the conversion, but tends to reduce the selectivity marginally. Higher catalyst loading improves the conversion with marginal rise in selectivity. Thus, calcium oxide can be effectively used as a heterogeneous catalyst in the current scheme involving anthranilate-trimethylcyclohexanol. The transesterification strategy is also green, since it eliminates the

neutralization step, which is required in case of esterification reaction catalyzed by homogeneous catalyst.

Acknowledgements The authors are thankful to the Indian Institute of technology, Mumbai, for the support provided for the FT-IR, ^{13}C NMR, ^1H NMR, TPD, Mass, Elemental, and Image analyses.

References

- Abreu FR, Alves MB, Macêdo CCS, Zara LF, Suarez PAZ (2005) New multi-phase catalytic systems based on tin compounds active for vegetable oil transesterification reaction. *J Mol Catal A Chem* 227:263–267. doi:10.1016/j.molcata.2004.11.001
- Billman JH, Smith WT Jr, Rendall JL (1947) Anticonvulsants. Esters of γ -diethylamino- α -phenylbutyric acid. *J Am Chem Soc* 69:2058. doi:10.1021/ja01200a070
- Blandy C, Gervais D, Pellegatta JL, Gillot B, Guiraud R (1991) Stearic acid esterification catalysed by titanates: comparative study of homogeneous and heterogeneous systems. *J Mol Catal* 64:L1–L6. doi:10.1016/0304-5102(91)85117-K
- Boeya P-L, Maniama GP, Hamid SA (2011) Performance of calcium oxide as a heterogeneous catalyst in biodiesel production: a review. *Chem Eng J* 168:15–22. doi:10.1016/j.cej.2011.01.009
- Brenner M, Huber W (1953) Preparation of α -amino acid esters by alcoholysis of the methyl ester. *Helv Chim Acta* 36:1109. doi:10.1002/hlca.19530360522
- Dan C, Popovici E-J, Ungur L, Pascu L, Ciocan C, Grecu R (2001) Spectroscopic characterisation of precursors for calcium hydroxide synthesis. *Stud Univ Babeş-Bolyai Phys (Special issue):*417–422
- Frank RL, Davis HR Jr, Drake S, McPherson JB Jr (1944) Ester Interchange by Means of the Grignard Complex. *J Am Chem Soc* 66:1509. doi:10.1021/ja01237a027
- Galmarini S, Aimable A, Ruffray N, Bowen P (2011) Changes in portlandite morphology with solvent composition: Atomistic simulations and experiment. *Cem Concr Res* 41:1330–1338. doi:10.1016/j.cemconres.2014.03.009
- Gambaro R, Villa C, Baldassari S, Mariani E, Parodi A, Bassi AM (2006) 3,3,5-Trimethylcyclohexanols and derived esters: green synthetic procedures, odour evaluation and in vitro skin cytotoxicity assays. *Int J Cosmet Sci* 28:439–446. doi:10.1111/j.1467-2494.2006.00343.x
- Haken JK (1966) Studies in trans-esterification. *J Appl Chem* 16:89. doi:10.1002/jctb.5010160304
- Hameedi BH, Lai LF, Chin LH (2009) Production of biodiesel from palm oil (*Elaeis guineensis*) using heterogeneous catalyst: an optimized process. *Fuel Process Technol* 90:606–610. doi:10.1021/ef8007954
- He M, Xiao B, Liu S, Hu Z, Guo X, Luo S, Yang F (2010) Syngas production from pyrolysis of municipal solid waste (MSW) with dolomite as downstream catalysts. *J Anal Appl Pyrolysis* 87(2):181–187. doi:10.1016/j.jaap.2009.11.005
- Imwinkelried R, Schiess M, Seebach D (1987) *Org Synth* 65:230. doi:10.15227/orgsyn.065.0230
- Jitputti J, Kitiyanan B, Rangsunvigit P, Bunyakiat K, Attanatho L, Jenvanitpanjakul P (2006) Transesterification of crude palm kernel oil and crude coconut oil by different solid catalysts. *Chem Eng J* 116:61–66. doi:10.1016/j.cej.2005.09.025
- Kim HJ, Kang BS, Kim MJ, Park YM, Kim DK, Lee JS, Lee KY (2004) Transesterification of vegetable oil to biodiesel using heterogeneous base catalyst. *Catal Today* 93–95:315–320. doi:10.1016/j.cattod.2004.06.007

- Kontoyannis CG, Vagenas NV (2000) Calcium carbonate phase analysis using XRD and FT-Raman spectroscopy. *Analyst* 125:251–255. doi:[10.1039/A908609I](https://doi.org/10.1039/A908609I)
- Kouzu M, Hidaka J-S (2012) Transesterification of vegetable oil into biodiesel catalyzed by CaO: a review. *Fuel*. 93:1–12. doi:[10.1016/j.fuel.2011.09.015](https://doi.org/10.1016/j.fuel.2011.09.015)
- Leclercq E, Finiels A, Moreau C (2001) Transesterification of rapeseed oil in the presence of basic zeolites and related solid catalysts. *J Am Oil Chem Soc* 78:1161–1165. doi:[10.1007/s11746-001-0406-9](https://doi.org/10.1007/s11746-001-0406-9)
- Otera J, Yano T, Atsuya K, Nozaki H (1986) Novel distannoxane-catalyzed transesterification and a new entry to α,β -unsaturated carboxylic acids. *Tetrahedron Lett* 27:2383. doi:[10.1016/S0040-4039\(00\)84535-9](https://doi.org/10.1016/S0040-4039(00)84535-9)
- Rehberg CE, Fisher CH (1947) Preparation and polymerization of acrylic esters of olefinic alcohols. *J Org Chem* 12:226. doi:[10.1021/jo01166a004](https://doi.org/10.1021/jo01166a004)
- Rossi RA, de Rossi RH (1974) Preparation of benzoate esters of tertiary alcohols by transesterification. *J Org Chem* 39:855. doi:[10.1021/jo00920a030](https://doi.org/10.1021/jo00920a030)
- Seebach D, Hungerbühler E, Naef R, Schnurrenberger P, Weidmann B, Züger M (1982) Titanate-mediated transesterifications with functionalized substrates. *Synthesis* 138. doi:[10.1055/s-1982-29718](https://doi.org/10.1055/s-1982-29718)
- Sercheli R, Vargas RM, Sheldon RA, Schuchardt U (1999) Guanidines encapsulated in zeolite Y and anchored to MCM-41: synthesis and catalytic activity. *J Mol Catal A Chem* 148:173–181. doi:[10.1016/S1381-1169\(99\)00054-0](https://doi.org/10.1016/S1381-1169(99)00054-0)
- Taft RW Jr, Newman MS, Verhoek FH (1950) The Kinetics of the Base-catalyzed Methanolysis of Ortho, Meta and Para Substituted 1-Menthyl Benzoates. *J Am Chem Soc* 72:4511. doi:[10.1021/ja01166a048](https://doi.org/10.1021/ja01166a048)
- Verziu M, Florea M, Simon S, Simon V, Filip P, Parvulescu VI, Hardacre C (2009) Transesterification of vegetable oils on basic large mesoporous alumina supported alkaline fluorides—evidences of the nature of the active site and catalytic performances. *J Catal* 263:56–66. doi:[10.1016/j.jcat.2009.01.012](https://doi.org/10.1016/j.jcat.2009.01.012)
- Watcharathamrongkul K, Jongsomjit B, Phisalaphong M (2010) Calcium oxide based catalysts for ethanolysis of soybean oil Songklanakarin. *J Sci Technol* 32(6):627–634
- Wulfman DS, McGiboney B, Peace BW (1972) Preparation and use of t-butyl esters: selective transesterification. *Synthesis* 49. doi:[10.1055/s-1972-21832](https://doi.org/10.1055/s-1972-21832)
- Xie W, Peng H, Chen L (2006) Transesterification of soybean oil catalyzed by Potassium loaded on alumina as a solid-base catalyst. *Appl Catal A Gen* 300:67–74. doi:[10.1016/j.apcata.2005.10.048](https://doi.org/10.1016/j.apcata.2005.10.048)
- Zhang S, Zu YG, Fu YJ, Luo M, Zhang DY, Efferth T (2010) Rapid microwave-assisted transesterification of yellow horn oil to biodiesel using a heteropolyacid solid catalyst. *Bioresour Technol* 101:931–936. doi:[10.1016/j.biortech.2009.08.069](https://doi.org/10.1016/j.biortech.2009.08.069)